

1. Introduction

It is well-known that block copolymers consisting of incompatible components form ordered self-assembled structure, so-called microphase-separated structure in bulk state.[1]-[4] The phase-separated domains obtained by block copolymers self-assembly corresponds to the size of the polymer (degree of polymerization), which can be controlled during the synthesis of the constituent blocks.

Using the characteristic of the block copolymers, they are considered to be utilized in many fields, e.g. material for bioscience, electric devices, chemical processing devices and lithography.

Block copolymer nanolithography, also known as directed self-assembly (DSA), is an essential technology for next generation lithography to achieve nanoscale-, and cost-effective patterning.[5]-[8]

A microphase-separated structure with the half pitch pattern formation around 10nm has been already accomplished to combine DSA with conventional lithography technique. The size and the resolution of the pattern are closely related to the size and chemical composition of the block copolymers. The next target for the microscopic patterning using block copolymers is to form the microphase-separated structure with the half pitch less than 10 nm. For this purpose, precise synthesis such as living anionic polymerization has been utilized.

In previous 30 years, fundamental and applied works concerning block copolymers using living anionic polymerization have been remarkably progressed. Various kinds of multi block copolymer such as ABCA[9], ABCD[10], ABC star[11]-[15], ABn miktoarm copolymers[16], and etc. were synthesized for the morphological study for the academic viewpoints.

Furthermore the functional polymeric materials from the multiblock copolymers have been also prepared for the industrial viewpoint, that is, preparation of charge-mosaic membrane from BABCA pentablock copolymers by Fujimoto et al. [17]-[21] and fabrication of solid polymer electrolyte from block-graft copolymers by Hirahara et al. [22]-[28] was one of the outstanding examples of the frontier works using living anionic polymerization technique.

Recently using highly-skilled living anionic polymerization techniques, we have successfully synthesized diblock copolymers with low molecular weight, and the obtained block copolymer has formed the definite microphase-separated structure (alternative lamellar structure) with the half pitch of less than 10nm.[29]-[39] However the formation of the microphase-separated structure with the narrower half pitch (less than 5.0nm) by the same diblock copolymers should be difficult. Because the interaction parameter, χ , of two blocks is relatively low, the block copolymers tend to become miscible. So, we have attempted to synthesize block copolymer consisting of strong segregated components (high χ) and furthermore to use multiblock copolymers such as ABA-type and ABAB-type instead of the simple AB diblock copolymer to solve the problem.

Furthermore, we have developed advanced large-scale living anionic polymerization apparatus to prepare the well-defined multiblock copolymers scaled over 3Kg.

2. Example of previous work

Charge mosaic membrane is made of Poly(Isoprene-*block*-Styrene-*block*-Butadiene-*block*-Amine-*block*-Isoprene) synthesized by anionic polymerization, the polyamine moiety is then quaternization, and the polydiene moiety is cross-linked. Finally, the polystyrene moiety was sulfonated. Figure 1 shows a schematic diagram of the tetrablock polymer, a transmission electron microscope (TEM), and a diagram of the principle of ion transmission, showing that the cation exchange layer and anion exchange layer, which are separated from each other by an insulating layer, are arranged in regular alternation. The principle of ion transmission is described in detail in MEMBRANE, 8(4), 212-224 1983 and MEMBRANE, 16(4), 233-238 1991 (Miyaki et. al.).

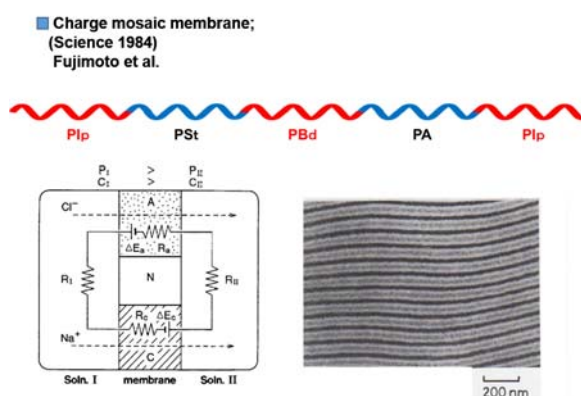


Figure 1. Charge mosaic membrane

The liquid crystal polymer in Figure 2 is made by coupling a small molecule liquid crystal to Poly(*p*-hydroxystyrene), the central chain of Poly(Styrene-*b*-*p*-Hydroxystyrene-*b*-Styrene). It can be used as a reversible recording medium because fine dots can be formed or disappeared at any position by irradiation of laser light. Incidentally, the coupling rate of small molecule liquid crystals is 100%. This method covers the disadvantage of anionic polymerization that the number of polymerizable monomers is small. We have synthesized DDS, oxygen-enriched membranes, hemicellulose blockpolymers, peptide polymers, water filtration membranes, etc. The coupling method is one of the most important synthetic methods because it can easily create functional polymers by simply changing materials.

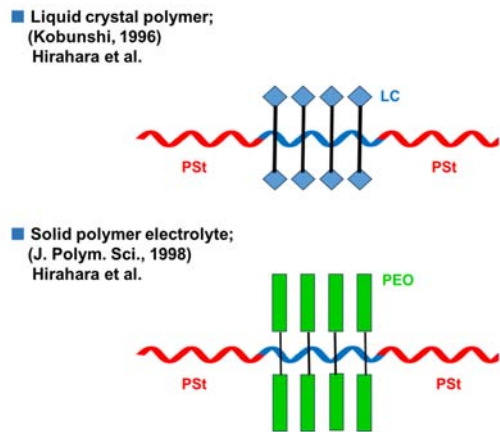


Figure 2. Schematic diagram of liquid crystal polymer and solid polymer electrolytes.

Solid polymer electrolyte was obtained by grafting ethylene oxide from PHSt, the central chain of P(St-*b*-HSt-*b*-St), by the growth method. We call this polymer a block-graft copolymer (TGE). Despite the total molecular weight reaching 40×10^4 , the PDI (GPC) = 1.08 was very sharp. Figure 3 shows a schematic diagram of a solid polymer electrolyte, with PSt as the sphere and PEO (polyethylene oxide) as the matrix, where PSt and PEO chains are responsible for the mechanical strength and ionic conductivity of the membrane, respectively.

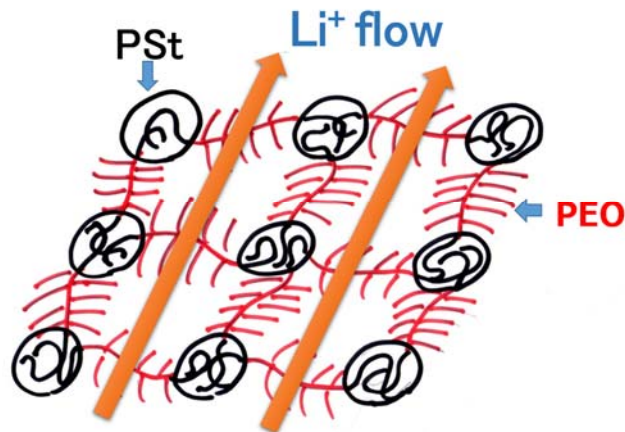


Figure 3. Schematic diagram of the solid polymer electrolyte

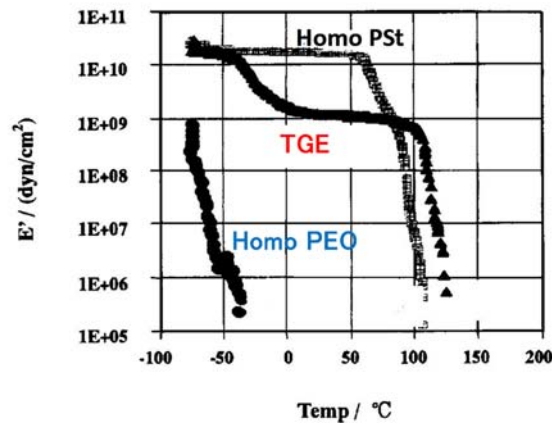


Figure 4. Temperature dependence of the storage modulus

Homopolymer of PSt exhibits high E' from -60°C to $+70^{\circ}\text{C}$, but decreases rapidly from around T_g (glass transition temperature). Low molecular weight PEO is liquid at room temperature, so there is no E' . On the other hand, TGE exhibits a high mechanical strength of $1\text{E}+9$ up to around $+110^{\circ}\text{C}$, even though the PEO chains in the liquid state form a matrix. Block copolymers have two T_g , and TGE also has a PEO T_g around -40°C and a PSt T_g around $+110^{\circ}\text{C}$ observed. This is one of the reasons for the high ionic conductivity of this tough film. (Figure 4) Furthermore, when TGE was impregnated with an electrolyte to produce a semi solid polymer electrolyte, the ionic conductivity was increased more than 1000 times without much loss of film strength.

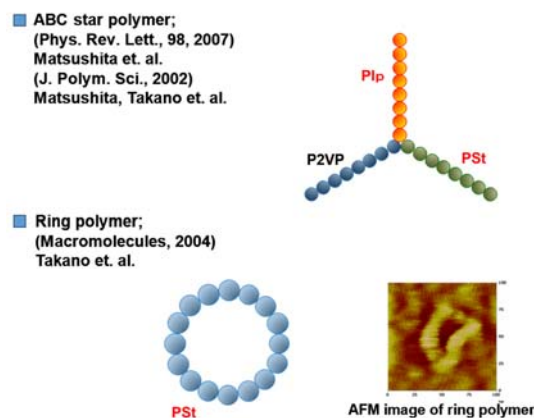


Figure 5. ABC star polymer and ring polymer

Matsushita et al. realized quasicrystalline structures in polymers by self-assembling ternary

star polymers composed of Polystyrene, Polyisoprene, and Poly(2-vinylpyridine). [Figure 5]
Takano et al., synthesized and characterized in detail a ring polymer of PSt with a cyclization ratio as high as 95%. The AFM image was taken over 25 years ago, so the image is not very clear, but the shape of the ring polymer could still be clearly seen.

3. Relative evaluation method of block copolymers

Figure 6 shows a GPC chromatogram of a polymer, where M_n , M_w , M_z , and M_p are the number-average molecular weight, weight-average molecular weight, Z-average molecular weight and peak top, respectively. Here, N is the number of polymer molecules, M is the molecular weight, and C is the sample concentration, $C(\text{wt./vol.}) = M \cdot N$. M_n is the simple arithmetic mean, M_w is the weighted mean using molecular weight as a weight, and M_z is the weighted mean using the square of molecular weight as a weight. $M_w/M_n = \text{PDI}$ is used as an index to evaluate the spread of molecular weight (molecular weight distribution); the smaller the PDI, the narrower the molecular weight distribution.

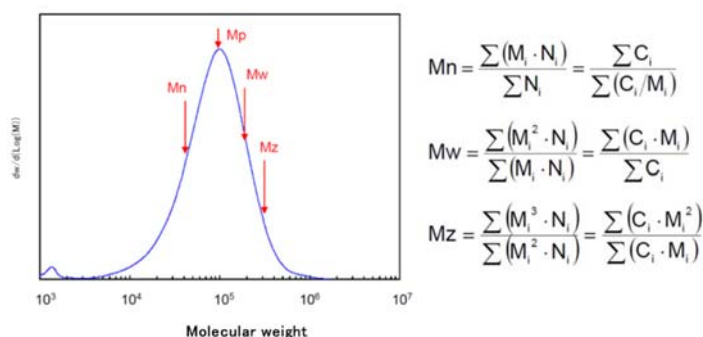


Figure 6. Definition of molecular weight distribution

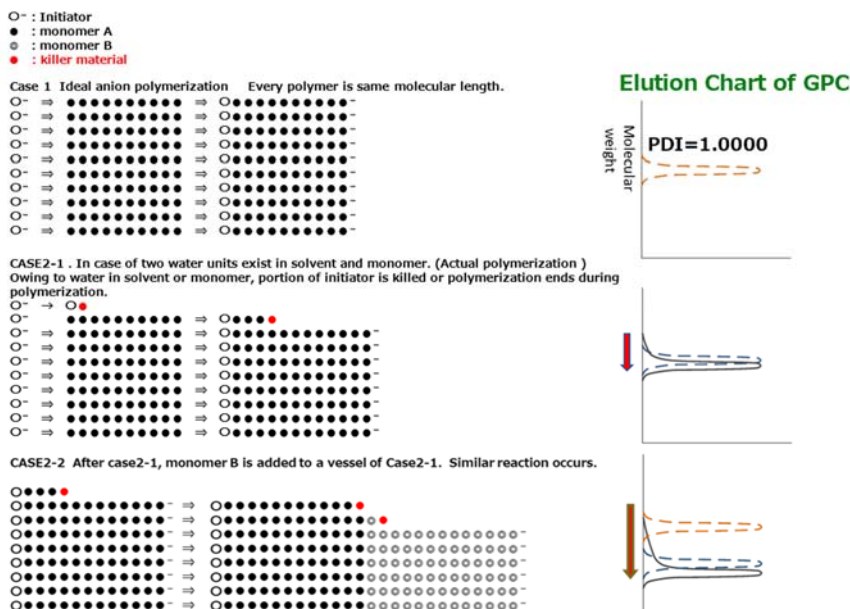


Figure 7. Why distribution of multiblock copolymer becomes wilder?

Figure 7 shows a schematic diagram of why the PDI becomes wider when block copolymers are synthesized by anionic polymerization. Case 1 is the polymerization under the so-called ideal

condition where there is no killer material at all in the reaction system. In this case, the initiator and the carbanion are not inactivated during the polymerization process, so the homopolymer with the designed molecular weight is obtained. The PDI is 1.0000, as in the case of homo polymer. In Case 2-1, the molecular weight of Polymer A is larger than the designed molecular weight because some initiators and the growing ends of the A chain are deactivated by the monomers, solvents, and a few killer materials present in the polymerization environment, resulting in a distribution.

Case 2-2 shows the polymerization of a diblock polymer. The unreacted killer material attacks the growing ends of the A chain and the growing carbanion of the B chain, causing the deactivated polymer to accumulate in the low molecular weight region. This eventually remains in the block copolymer and becomes a troublesome impurity.

4. Hypothesis of Defect Occurrence

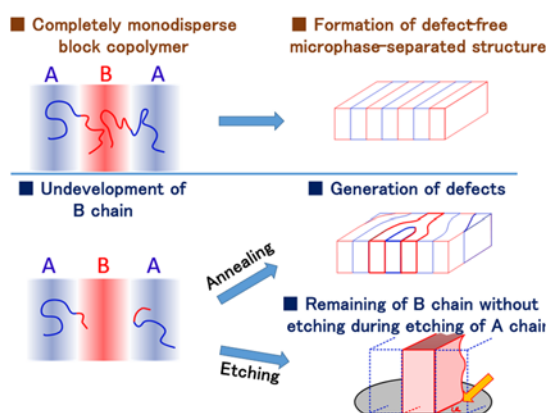


Figure 8. One hypothesis for the occurrence of defects

Figure 8 shows a schematic diagram of the reasons for the occurrence of defects. Please note that this is only a hypothesis. Suppose we have an AB block copolymer in an ideal state, which is microphase-separated in an ideal state, and a defect-free lamellar structure is formed. In reality, however, all block copolymers are distributed and contain impurities that have been killed during growth. If this is used for DSA, for example, there may be cases where immature B chains dissolve in the A chains. In the case of annealing, there is a possibility that defects may occur from this. On the other hand, if it is dry-etched, the B chain may remain on the substrate. Although this idea is still hypothetical at this point, we believe that this may be one of the causes of the occurrence of defects.

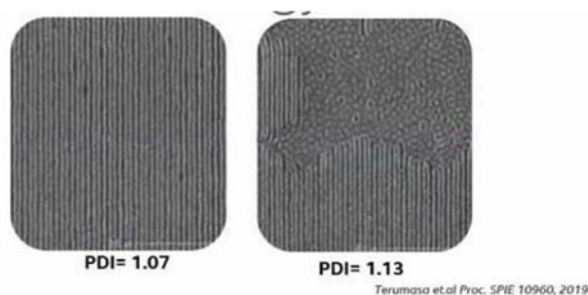


Figure 9. Relationship between PDI and defects (SEM)

Figure 9 shows the results of Kosaka et al. When block copolymers with the same molecular weight and composition but different PDI were coated on the substrate and annealed, those with PDI = 1.13 did not phase separate well. To further verify this result, we synthesized block copolymers with PDI = 1.5, 1.1, 1.05, and 1.01 with equal molecular weight and composition, and investigated the correlation between the number of defects and PDI in detail. If it is proven that the

number of defects decreases with decreasing PDI, it is concluded that PDI greater than 1.01 should not be used.

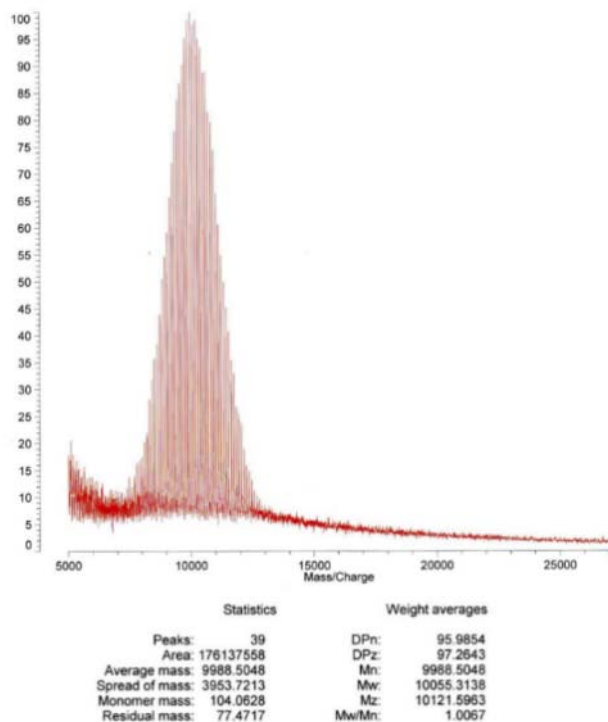


Figure 10. TOF-MS of monodisperse PS

Although GPC is an excellent method for determining the relative molecular weight or PDI of polymers, it does not accurately represent the molecular weight of block copolymers. This is because GPC is only a relative molecular weight based on standard PSt. For example, the results obtained vary greatly depending on the model of the equipment and the type, length, and number of separation columns. We have been focusing on this issue for a long time and have verified the results using six GPCs of different instrument manufacturers and models, and have confirmed that there is an error of ± 1000 for Mw and ± 0.1 for PDI.

Figure 10 shows the molecular weight of PSt measured by TOF-MS, one of the absolute molecular weight measurement methods, although the data is now 25 years old. PSt with Mw (GPC) = 10,000 and PDI (GPC) = 1.02, synthesized by anionic polymerization, was measured by TOF-MS, giving an Mw of 10,060 and a PDI (TOF-MS) of 1.007.

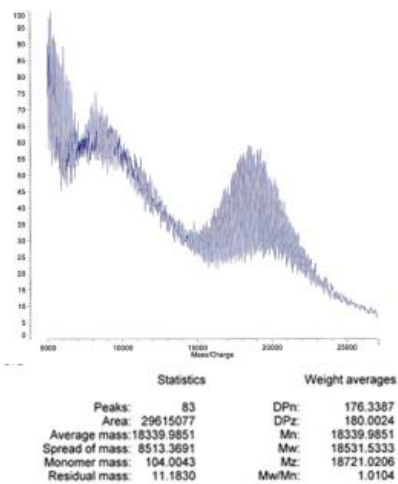


Figure 11. TOF-MS measurement of ring polymer

Figure 11 shows the TOF-MS results of the ring polymer shown in Figure 5. The values obtained by the membrane osmometry ($M_n = 18,300$, M_w (GPC) = 18,000, and PDI (GPC) = 1.01) were obtained as $M_w = 18,630$ and PDI = 1.01 by TOF-MS, although these values were also measured 25 years ago. The reason why the PDI (GPC) values did not differ from PDI (TOF-MS) compared to the linear polymer is not well understood.

5. Living anionic polymerization using breakable seal method



Figure 12. Glass processing

As Figure 12 shows how the polymerization equipment is assembled with a hand burner, anionic polymerization is usually performed using glass processing techniques, which require at least two to three years of training to master. This is a barrier to entry, and there are only a few anion polymerization researchers in the world. It is hell, especially during the hot summer months.

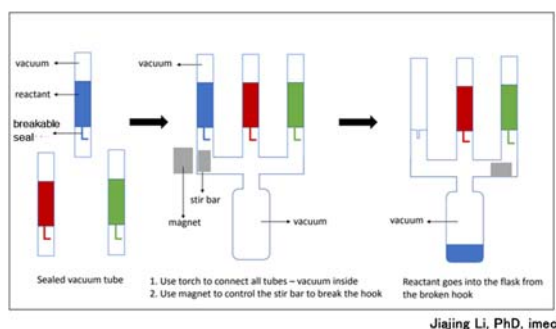


Figure 13-1. Living Anion Polymerization using Special Glassware.

The initiator, solvent, monomers, and polymerization stopper used in anionic polymerization are melt-sealed in a glass vessel fitted with a breakable seal. This is attached to the polymerization vessel, and the entire apparatus is maintained in a high vacuum by a diffusion pump or turbo molecular pump, in which anionic polymerization is performed. Polymerization is carried out by breaking down the breakable seal by moving the stir bar, which is placed inside the apparatus in advance, with a magnet outside. This allows anionic polymerization to be carried out while maintaining a high vacuum.

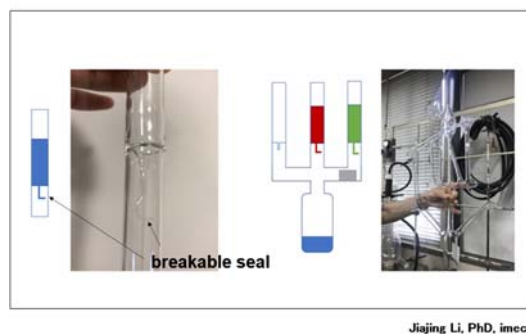


Figure 13-2. Special Glassware.

The hook-shaped glass shown in Figure 13-2 is a breakable seal. Anionic polymerization using this glass is called the breakable seal method, and is one of the most important techniques for anionic polymerization researchers. On the other hand, it is not easy to make a breakable seal that does not break during various operations but breaks reliably when necessary, and it requires considerable effort, patience, and discipline to be able to make it by oneself.

6. The challenge of HVM (High-Volume Manufacturing)



Figure 14. 5L scale polymerization apparatus

Anionic polymerization using the breakable seal method is a rare method that can synthesis polymers with molecular weight, molecular structure and sharp PDI according to molecular design, but it is difficult to synthesis a large number of samples. Therefore, we developed a 5L-scale polymerization apparatus consisting of SUS316L (composite electropolished) and QVF glass as a preliminary step for mass production and attempted to synthesis DSA. Figure 14 shows a part of the apparatus, which is a completely original product designed and manufactured by me. All parts are standardized and communized, so as long as you can tighten the bolts and nuts, you can learn anionic polymerization technology in about a month. The specifications of the equipment are (1) attainable vacuum $< 1 \times 10^{-6}$ Pa and (2) helium leak rate $< 5 \times 10^{-9}$ atm.cc/sec. (2) means that if the inside of the polymerization equipment is sealed in a vacuum, it would take more than 3000 years for 1 cc of air to leak in from outside the equipment.

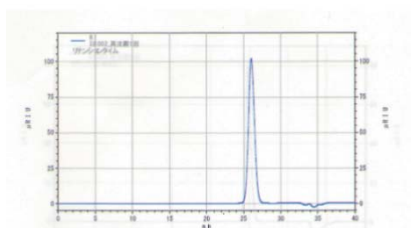


Figure 15. GPC chart of P(St-*b*-BuOSt)

Anionic polymerization using a 5L polymerize initially reached only about PDI = 1.1, but through two-step purification of the monomer and improvement of the equipment, it was able to reach a level

almost comparable to the breakable seal method. Currently, we are making efforts to increase the polymerization concentration to 30% or more in order to raise the pot yield. Incidentally, 5% is the standard for the breakable seal method.

Figure 15 shows an experimental synthesis of P(St-*b*-BuOSt), where a polymer with $M_w=10,000$ and $PDI=1.02$ can now be synthesized reproducibly. Incidentally, $PDI(GPC) = 1.02$ corresponds to $PDI < 1.003$ in MALS and TOF-MS. In the future, we would like to adopt the absolute molecular weight value.

7. Examples of DSAs we have synthesized so far

We have synthesized a number of block copolymers, some of which are shown in Figures 16-1 and 16-2. PMMA is Poly(methyl methacrylate), PX is a silicon-containing polymer, P α MSt is Poly(α -methyl styrene), PBuOSt is Poly(*p*-butoxy styrene), and PBuSt is Poly(*p*-4-butenyl styrene).

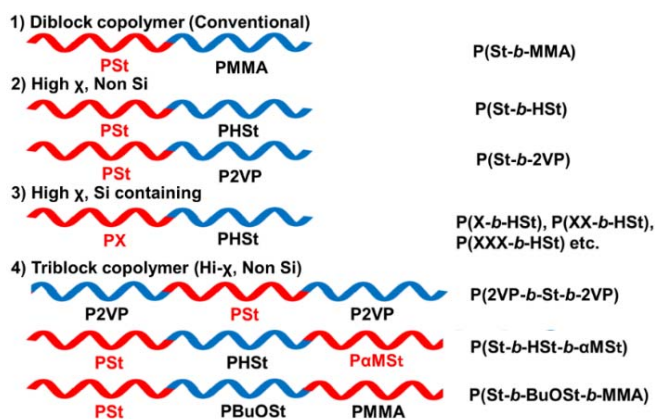


Figure 16-1. DSA synthesized so far

1) is an old type of diblock copolymer that has been the subject of most research reports. Since MMA, a polar monomer, is used as one component, polymerization is difficult, and the PDI is not so small. 2) to 9) are high-chi di- to octablock copolymers, and are further distinguished by the presence or absence of silicon in the polymer.

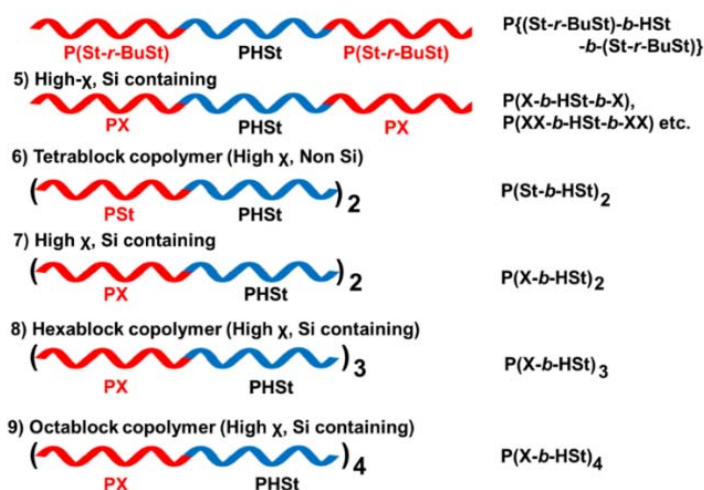


Figure 16-2. DSA synthesized so far

8. Synthesis and characterization of DSA

8-1. Synthesis and Characterization of PSt-*b*-PMMA

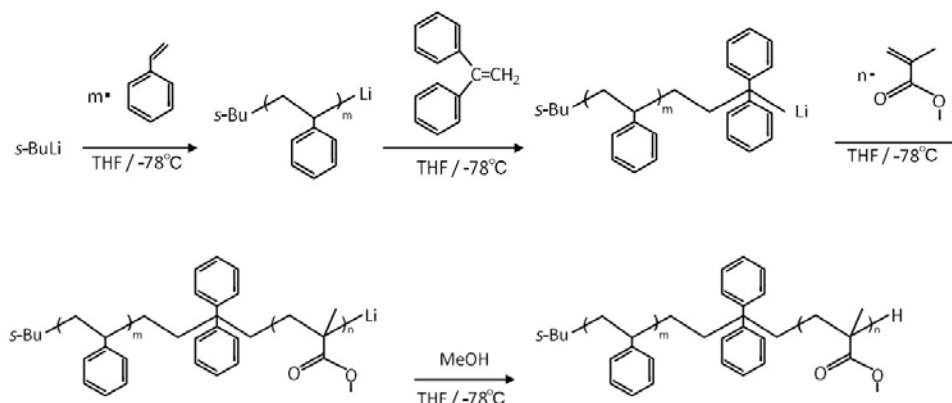


Figure 17. Polymerization scheme for P(St-*b*-MMA).

Polystyrene-*block*-polymethyl methacrylate (PSt-*b*-PMMA) has been extensively studied because of the similar surface energies of the PSt and the PMMA blocks, which leads to the perpendicular orientation upon simple thermal annealing without neutral layer. However, it was reported that the resolution limit was 13 nm half pitch (hp) and a lower dry etch selectivity (2:1). To achieve sub-10 nm feature size, we synthesized PS-*b*-PMMA with the narrow molecular weight distribution ($M_w/M_n < 1.1$), and the composition PS = 0.5 by the living anionic polymerization technique. The domain spacing (D) of alternative lamellar structure of the obtained sample with molecular weight of 25k was determined to be 20.5 nm ($hp = D/2 = 10.3$ nm) by SAXS measurement (Figure 1-a). It was confirmed that the hp is smaller than the resolution limit of PSt-PMMA predicted previously¹.

Figure 17 shows the polymerization scheme of P(St-*b*-MMA). polymerization of P(St-*b*-MMA) itself is simple, but it is difficult to monodisperse MMA, a polar monomer, and the PDI was only 1.04 even using the breakable method.

Table 1. Morphological observation and quantitative analysis of domain size.

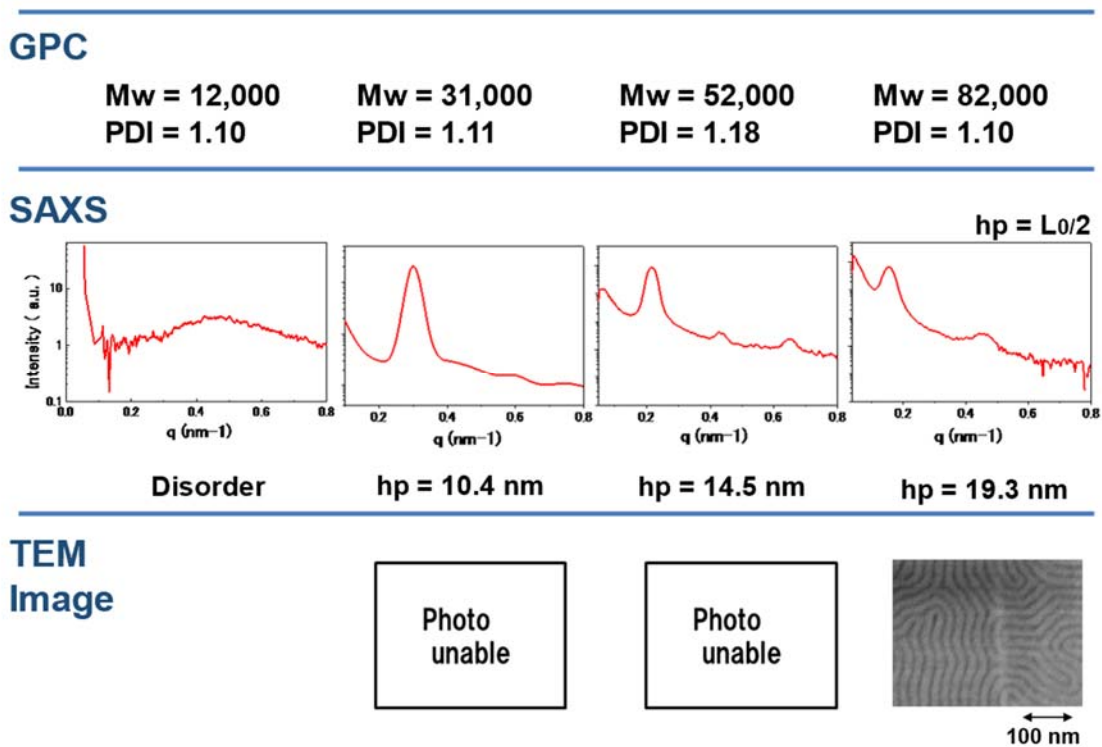


Table 1 shows the Mw, PDI, SAXS, and TEM results for P(St-*b*-MMA). Here, SAXS was measured using a Spring 8 (Riken) GI-SAX; TEM was obtained by staining samples with OsO₄ or RuO₄. Although the PDI is not so good since this data is about 10 years old, SAXS and TEM observations still confirmed the formation of a clear microphase-separated structure.

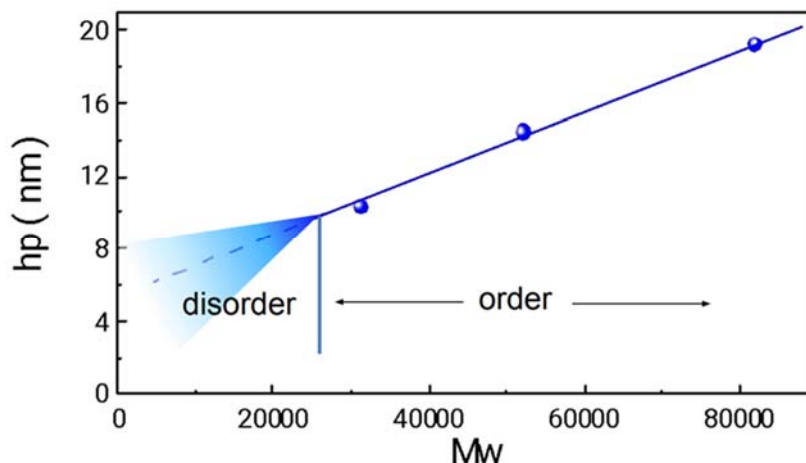


Figure 18. hp vs. Mw(Lamellar structure)

Figure 18 plots hp versus Mw in Table 1, showing a clean linearity between Mw and hp. On the other hand, it was found that PSt and PMMA compatibilizer with each other around hp of 10 nm,

forming a microphase-separated structure down to a smaller region than the theoretical calculation results.

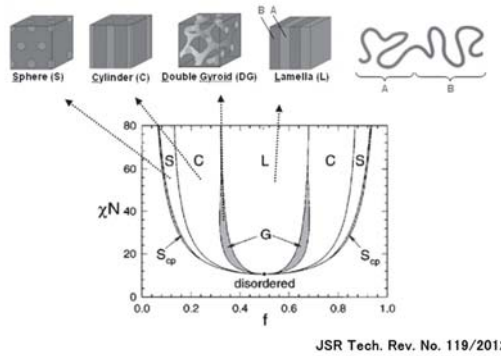


Figure 19. A representation of the equilibrium microdomain structures of linear diblock copolymer

Diblock copolymers, in which two mutually incompatible polymer components are covalently linked, form a microphase separation by intermolecular assembly of the same polymers. In this process, the interfacial curvature at the time of assembly changes according to the molecular chain length ratio f between the two polymer components. As a result, regular morphologies such as spherical, cylinder, gyroid, and lamellar structures are formed (Figure 19). These regular structures can be applied to semiconductor fine patterning. On the other hand, there is a limit to how much the molecular weight can be lowered, and eventually the material will become miscible; for P(St-*b*-MMA), this limit is around 10 nm.

Directed Self-Assembly (DSA) of block copolymers (BCPs) is one of the candidates for the next generation technique for semiconductor patterning at the length scale in sub10 nm regime. Polystyrene-*block*-polymethyl methacrylate (PSt-PMMA) has been extensively studied because of the similar surface energies of the PSt and the PMMA blocks, which leads to the perpendicular orientation upon simple thermal annealing without neutral layer. However, it was reported that the resolution limit was 13 nm half pitch (hp) and a lower dry etch selectivity (2:1). To achieve sub-10 nm feature size, we synthesized PS-*b*-PMMA with the narrow molecular weight distribution ($M_w/M_n < 1.1$), and the composition PS = 0.5 by the living anionic polymerization technique. The domain spacing (D) of alternative lamellar structure of the obtained sample with molecular weight of 25k was determined to be 20.5 nm ($hp = D/2 = 10.3$ nm) by SAXS measurement (Table 1). It was confirmed that the hp is smaller than the resolution limit of PSt-PMMA predicted previously¹.

8-2. New concept polymer: random-block copolymers

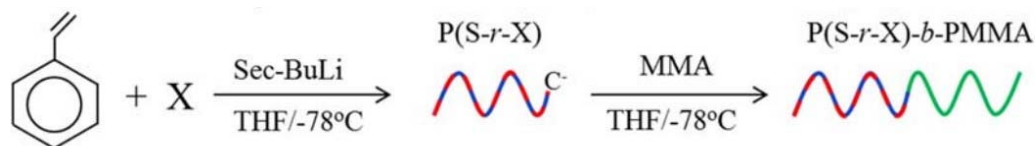


Figure 20. New concept copolymer

We synthesized a series of poly(styrene-*random-X*)-*block*-polymethyl methacrylate P(S-*r-X*)-*b*-PMMA where X means Silicone containing monomer. One of the P(S-*r-X*)-*b*-PMMA sample showed narrow domain spacing of 20.0 nm (10.0 nm hp) by SAXS measurement (Figure 20).

For the evaluation of the dry etch selectivity, PMMA, PS and also P(St-*r-X*) with various compositions were synthesized. As a result, the etch selectivity of P(S-*r-X*) with a certain composition was estimated to be over three times higher than that for PMMA (Figure 24).

Investigation of the BCPs with narrower half pitch and a higher dry etch selectivity is still going on.

Table 2. Molecular weight, PDI (GPC) and composition ratio of P(St-*r-X*)-*b*-PMMA

1. P(St-*b*-MMA)

5 Mn = 30,000, PDI = 1.1, PSt : MMA = 50 : 50(1H-NMR)

2. P(St-*r-X*)-*b*-PMMA

1 (X35) Mn = 26,000, PDI = 1.16, PSt : X : PMMA = 33.6 : 16.3 : 50.1

2 (X10) Mn = 30,000, PDI = 1.05, 50.8 : 6.9 : 42.2

3 (X30) Mn = 28,000, PDI = 1.06, 33.4 : 16.8 : 49.8

4 (X20) Mn = 29,000, PDI = 1.06, 39.1 : 11.9 : 49.0

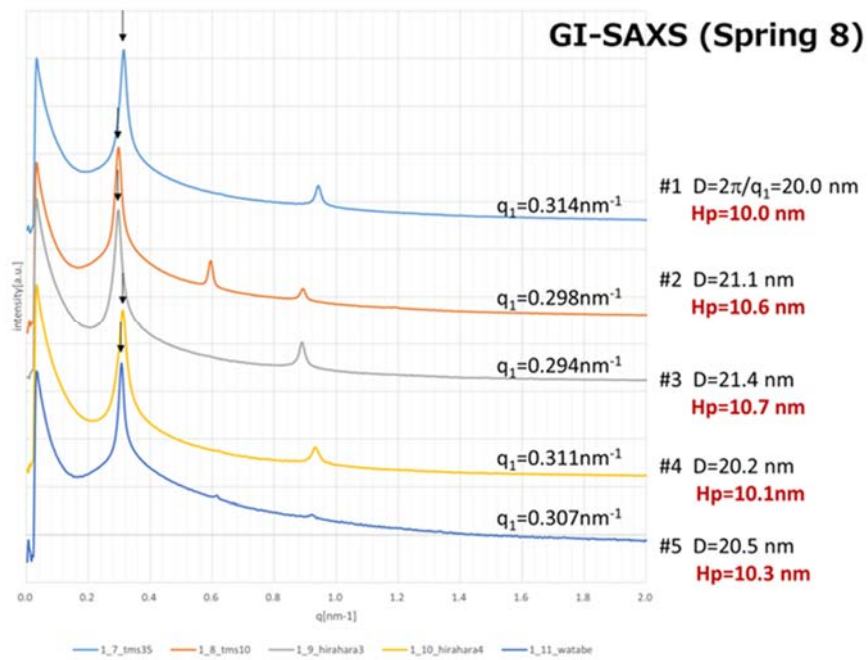


Figure 21. GI-SAX of P(St-*ran-X*)-*b*-PMMA

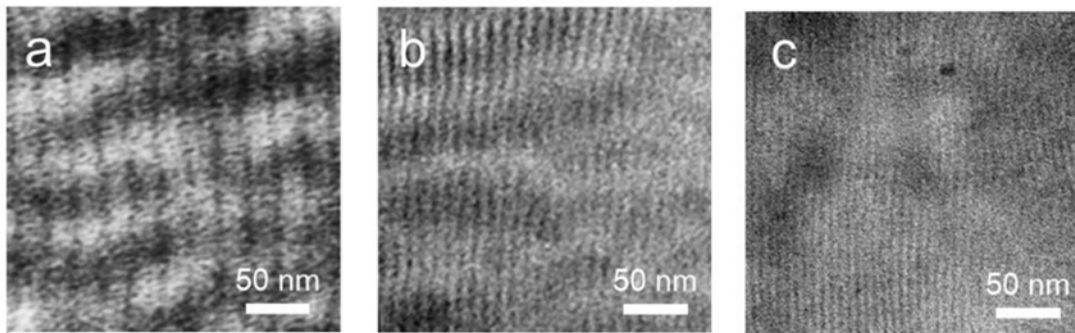


Figure 22. TEM photograph of P(St-*ran-X*)-*b*-PMMA.

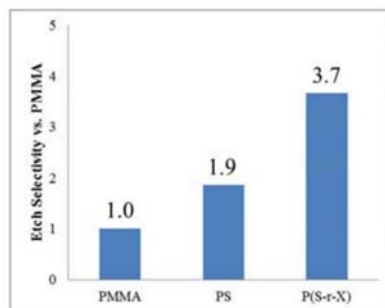


Figure 23. Etching ratio

Investigation of the BCPs with narrower half pitch and a higher dry etch selectivity is still going on.

8-3. AB diblock copolymer and ABAB tetrablock copolymer

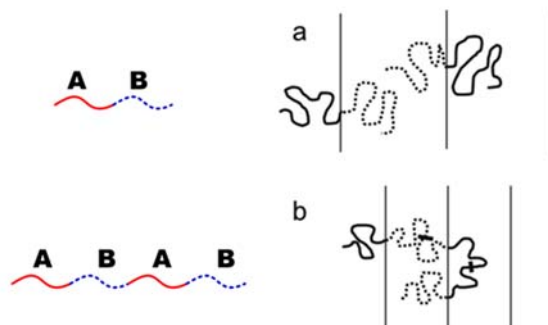
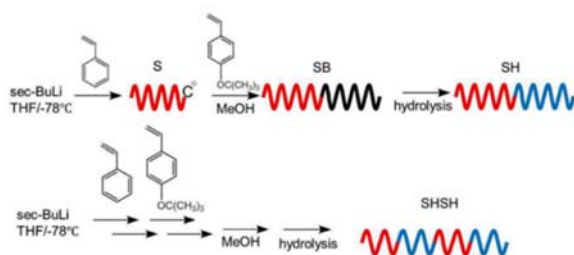


Figure 24. Schematic illustration of the chain conformation in comparison between (a) AB diblock copolymers and (b) ABAB tetrablock copolymers.

To prepare the narrower domain of microphase-separated structure by block copolymers, utilization of multiblock copolymer effective. In the case of AB diblock copolymer, the diblock copolymers have only end blocks that always take *tail* conformation, while multiblock copolymers such as ABAB have a middle block that can take either a *loop* and *bridge* conformation. Comparing between the chain dimension of a *tail* conformation and that of *loop/bridge* conformation with the same molecular weight, the latter should be smaller than the former. Accordingly, the domain spacing of multiblock copolymer with many block number should be shorter than that for simple diblock copolymer as shown in Figure 24.

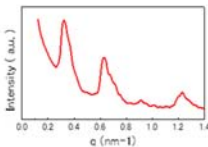
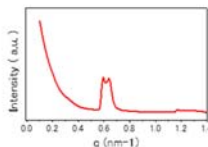
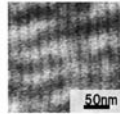
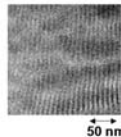


Scheme 1. Synthetic scheme of SH and SHSH block copolymers.

Block copolymers were synthesized by living anionic polymerization by multi-step sequential monomer addition in tetrahydrofuran with *sec*-BuLi as initiator at -78°C under vacuum or argon atmosphere. After being quenched with methanol, the obtained polymer was precipitated in excess

amount of methanol, and freeze-dried. Poly(4-*tert*-butoxystyrene) (B) was transformed into Poly(4-hydroxystyrene) by hydrolysis with hydrochloric acid in solvent. Example of the synthetic for SH diblock and SHSH tetrablock copolymer are shown in Scheme 1.

Table 3. Morphological observation and quantitative analysis of domain size.

	Diblock copolymer (SH)	Tetrablock copolymer (SHSH)
GPC	Mw = 27,000 PDI = 1.02	Mw = 27,000 PDI = 1.02
SAXS	 hp = 11.2 nm	 hp = 5.4 nm
TEM image		

8-4. Scontaining diblock copolymers and tetrablock copolymers

Table 4. Quantitative analysis of domain size. (diblock copolymers)

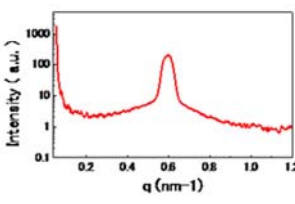
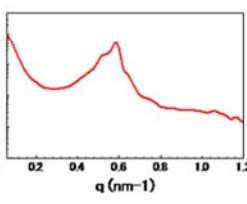
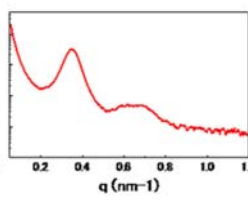
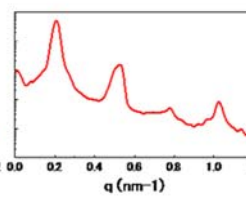
GPC	Mw = 4,000 PDI = 1.06	Mw = 6,000 PDI = 1.08	Mw = 7,000 PDI = 1.08	Mw = 9,000 PDI = 1.09
SAXS	 hp = 5.3 nm	 hp = 5.5 nm	 hp = 9.0 nm	 hp = 12.2 nm

Table 5. Quantitative analysis of domain size. (tetrablock copolymers)

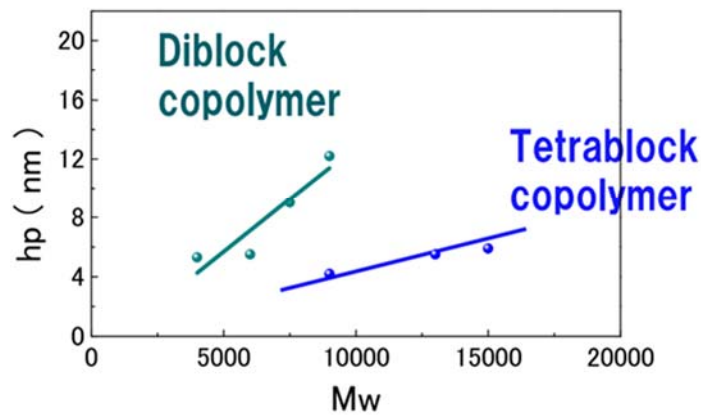
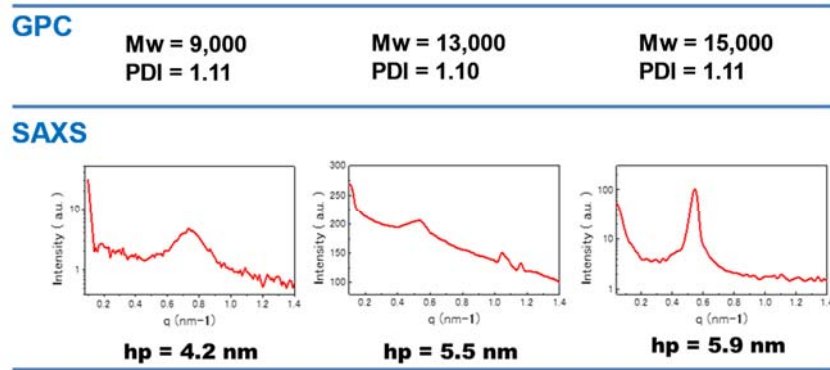


Figure 25. Comparison of diblock and tetrablock High-chi copolymers

Figure 25 compares the hp to Mw of diblock and tetrablock copolymers. The copolymers are the same High-chi polymers. Since the tetrablock slope is looser than the diblock slope, the different in hp is smaller even if the molecular weights of the polymer deviate slightly. Also, at the same molecular weight, the tetrablock exhibits a smaller hp. Which is an advantageous method for making micro-phase domains. (hp of less than 4nm may be achievable)

I have heard that devices manufactured using ASML's TWINSCAN NXE: 3400B (NA 0.33, wavelength 13.5 nm) have L/S and Ch of 15-25 nm. The latest High-NA 0.55 is said to have a

wavelength of 8 nm, but even so, it would be difficult to get L/S below 10 nm. (Figure 26)

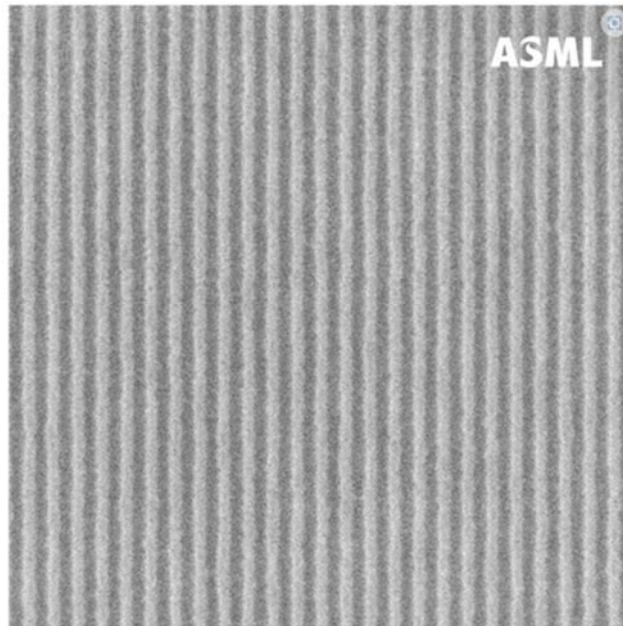


Figure 26. 10 nm L/S (ASML)

Furthermore, when it comes to High-NA 0.75, we do not know when the equipment will be ready. Our High-chi DSA reached hp 4.2 nm more than 8 years ago, and Sub 4 nm will be achieved soon. On the other hand, the words "3 nm generation" and "2 nm generation" are being bandied about without any clear evidence, but the actual L/S and Ch sizes are far from this. The DSA we have synthesized is an actual value measured by SEM, GI-SAXS, TEM, etc., so it is a reliable value. What generation should we call the hp = 4.2 nm that we have already achieved? I think it has reached a level that we can call 0.5 nm generation or 0.1 nm generation, but what do you think?

9. Further challenges for HVM

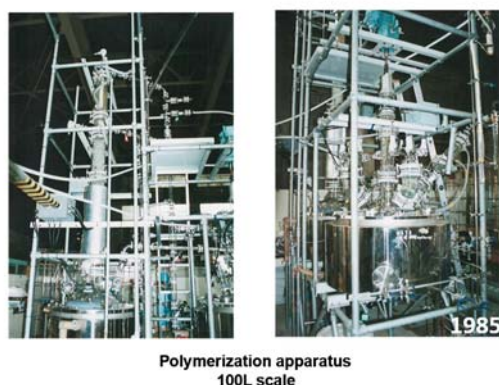


Figure27. Upscaling of Anionic Polymerization Equipment

The Teruo Fujimoto Laboratory at Nagaoka University of Technology has been working on increasing the size of anionic polymerization equipment since the early 1980s. The laboratory has successively installed and operated four large anionic polymerizers. The first was used for charge mosaic membrane, the second for oxygen-enriched films and monodisperse KrF resist, the third for functional paints with pigment binding sites, and the fourth for polymers for all-solid-state batteries. The second unit (Figure27) was constructed in 1985. The polymerization vessel was 100 L, and the distillation column was 5 m high, made of all QVF glass. The polymerization scale was normally 5Kg, and anionic polymerization up to 10 Kg could be performed. Incidentally, the second and fourth units were designed by me.



Figure 28. 30L Twin Reactor

Figure 28 shows the large-scale anionic polymerization apparatus. This apparatus consists of stainless steel reactor with high-speed rotating fin, electrical controller and turbo molecular vacuum pump. Attained evacuation of total system is $< 5 \times 10^{-5}$ Pa. Helium leak rate of total system is $< 5 \times 10^{-9}$ Pa \cdot m³/sec.

After setting of monomers, solvent, initiator and quencher to this apparatus, temperature and pressure can be controlled and multiblock copolymers with narrow molecular weight distribution are synthesized automatically. By using the apparatus, 3 kg of the block copolymer is synthesized in single batch. Incidentally, the equipment was designed and manufactured by us and is completely original.



Figure29. Twin Reactor rotating mechanism

The stirring blades inside the twin reactor are rotated by powerful magnets. The rotation speed can be set arbitrarily from 1~1000 rpm. A Tom and Jerry doll (Figure 29) is attached to the top of the magnets, which soothes the hearts of tired researchers on a daily basis. (Sometimes, it is replaced by the Jurassic Park version.)



Figure 30. Monomer container

The amount of monomer used for anionic polymerization is controlled using a precise electronic balance. The total weight of the monomer and the container containing the monomer can reach 10 kg, but the error in the amount of monomer to be fed is < 0.1 g. (Figure 30)



Figure 31. Continuous Polymerization Equipment

Figure 31 shows our newly designed and fabricated continuous anionic polymerization system. Although only homopolymers can be polymerized so far because they were originally developed for other applications; by continuously feeding monomers, hundreds of kilograms of polymer can be synthesized in a single day. If it is to be used for the production of base polymers for KrF resists, the quantity and quality will be satisfactory enough.

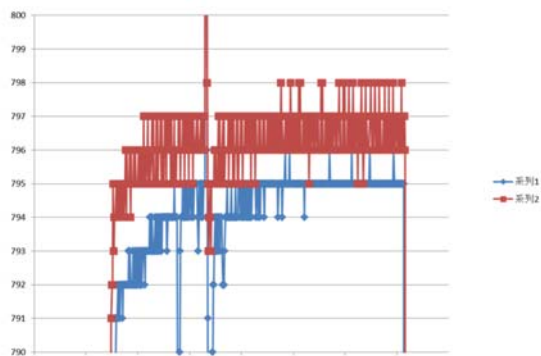


Figure 32. Raw material supply chart

Figure 32 shows the feed output of the continuous polymerize. The feed errors for both feed series 1 and 2 are $\pm 0.15\%$, which enables highly accurate polymerization. The system is equipped with a temperature sensor, pressure sensor, precision feed pump, precision balance, and Coriolis flowmeter. The inside of the apparatus is sealed with nitrogen gas, which has been approved by the fire department as an explosion-proof structure. A WD filter is installed on the left hand side of the apparatus to enable immediate re-precipitation of the polymer solution.

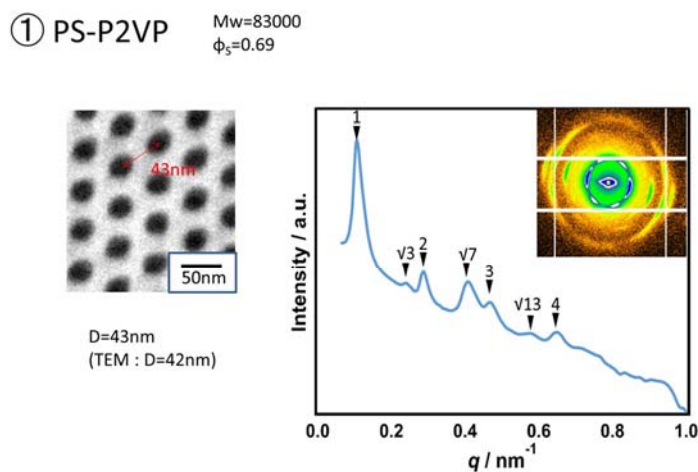


Figure 33. Assembly of continuous polymerization equipment

Figure 33 shows the fabrication of the continuous polymerization system. The equipment is completely original, and everything from design to assembly is done by our own hands. Although the number of team members is small, each of them is a highly specialized and capable person.

Our ultimate targets are ① the fabrication and operation of a large anionic polymerization system of 1000 L or more, and ② the development of a tabletop anionic polymerization system. It goes without saying that ① is a batch-type HVM system, but ② will be the ultimate continuous anion polymerization system. This equipment will continue to synthesize polymers continuously, and will continue to produce block copolymers at the same level as the batch type. Incidentally, the drawing of the apparatus has already been completed.

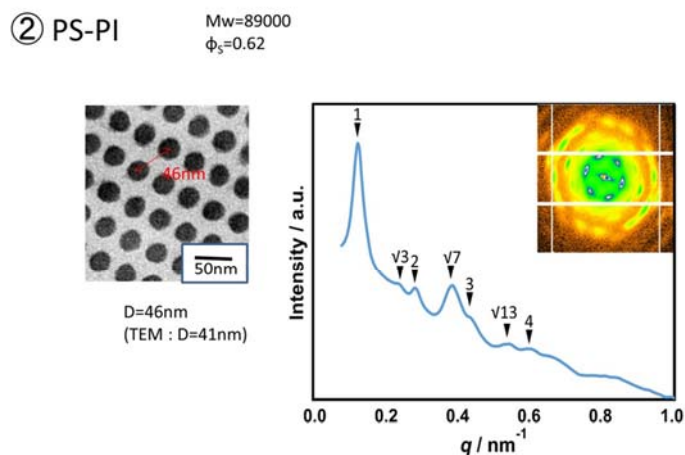
10. Other DSA



Takano et al.

Figure 34. TEM and GI-SAX of PSt-*b*-2VP

Figure 34 shows TEM images and SAX data of PSt-*b*-2VP, which was presented to several semiconductor manufacturers who requested DSA of about Ch = 50 nm.



Takano et al.

Figure 35. TEM and GI-SAX of PSt-*b*-PI

Figure 35 shows the data for PSt-*b*-PI; the inclusion of a rubber component in the DSA would make dry etching easier. On the other hand, when we tried to apply these data to conventional PSt-*b*-PMMA, we found that we needed $M_w = 1.8 \times 10^4$ to achieve Ch = 50 nm. When we actually made and supplied the polymer, it was highly evaluated.

11. Purification and trace analysis of DSA

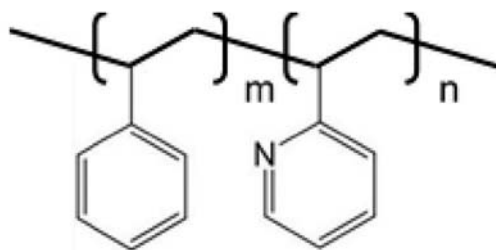


Figure 36. Structural formula of P(St-*b*-2VP)

In collaboration with Nippon Paul, we have purified P(St-*b*-2VP), a high-chi DSA, and analyzed its metal composition (Figure 37). (The polymer was synthesized by us (Figure 36), and its molecular weight and composition were $M_w=7930$ (MALS), PDI (GPC) = 1.07, and St : 2VP = 1:1.

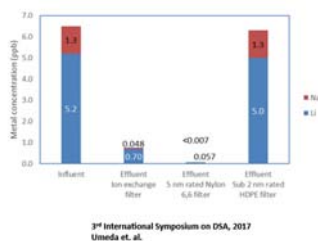


Figure 37. Single step filtration metal reduction

Metal concentration in P(St-*b*-2VP)/PGMEA solution before and after single step filtration. The Na and Li metals were drastically reduced after a single pass through a 5 nm Nylon 66 filter. (Figure 37) The final metal impurity content is shown in Summary.

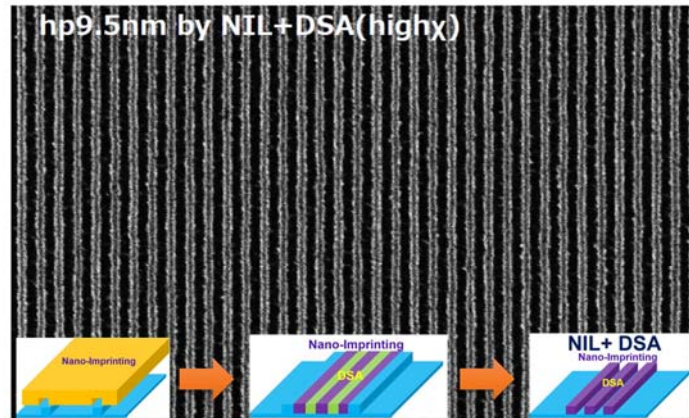
Summary

- **Single step filtration**
 - 5 nm rated Nylon 6,6 filter is most effective in comparison to ion exchange and sub 2 nm HDPE filters.
 - Li and Na levels were 0.057 ppb* and <0.007 ppb respectively.
- **Multi step filtration using ion exchange and 5 nm rated Nylon 6,6 filters**
 - Li and Na levels were reduced to <0.001 ppb and <0.01 ppb respectively.
 - Both molecular weight distribution and polymer concentration were not changed by filtration.

*: ppb=parts per billion (10⁻⁹)

PALL Corporation

12. NIL+DSA and EUV+DSA



Morita et al. SPIE. 9777, Alternative Lithographic Technologies VIII, 97770K

Figure 38. SEM photograph of NIL + DSA

Figure 38 shows the results obtained in collaboration with Toshiba Corporation. The DSA used is a Si-containing tetrablock copolymer, and the SEM photograph shows $hp = 9.5$ nm. In addition, DSA for 4.5 nm, 12 nm, and 50 nm were synthesized and examined for matching with NILs, and all showed good results. On the other hand, DSAs from $hp = 4$ to 20 nm have been developed for logic applications, and EUV + DSAs have been evaluated. Of particular note is $hp = 7$ nm. I dare not show SEM pictures here, but I have never seen such a beautiful L/S before. By the way, only about 20 people in the whole human race have seen this SEM photo. I don't know if I will show it to you all.

13. Intel's Position on EUV + DSA (cited material)

The figures in Figure 39-41 are taken from a paper presented by Chandra Sarna et al. of Intel at the 39th International Conference of Photopolymer Science and Technology, June 2022, Japan. Although we are astonished at and respect the high level of technology of Intel researchers, the data is not as good as the $hp = 7\text{ nm}$ data presented earlier. On the other hand, it is noteworthy that Figure 41 requirements for HVM. We have many years of accumulated DSA development technology and much knowledge about HVM, but unfortunately, we do not have the funds to build a factory for HVM. We would like to ask you, regardless of your nationality or the size of your company, to invest funds in us.

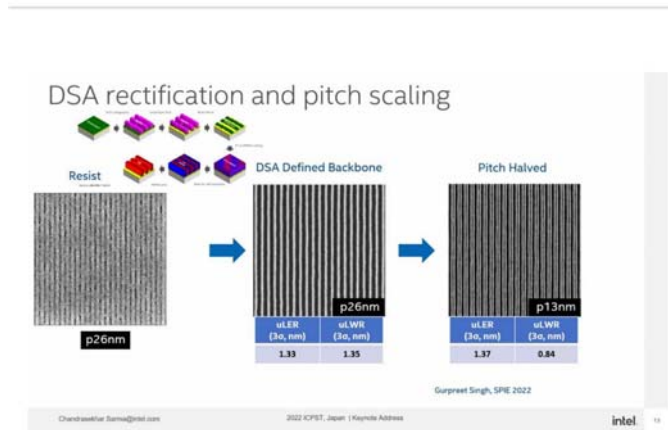


Figure 39. DSA rectification and pitch scaling

Multipitch DSA Strategy

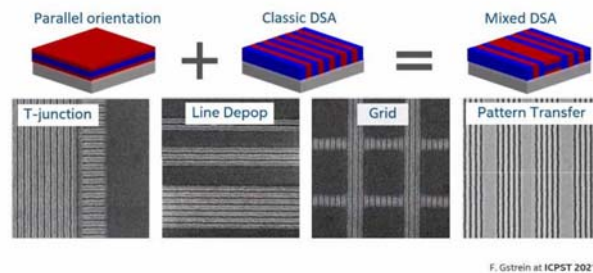


Figure 40. Multipitch DSA Strategy

DSA ECOSYSTEM INTERACTION

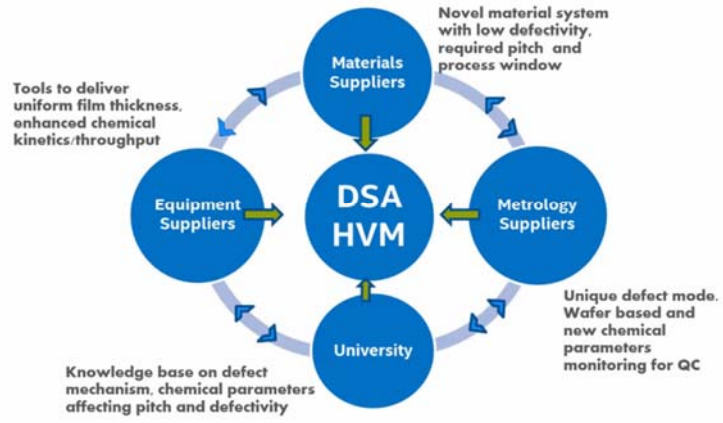
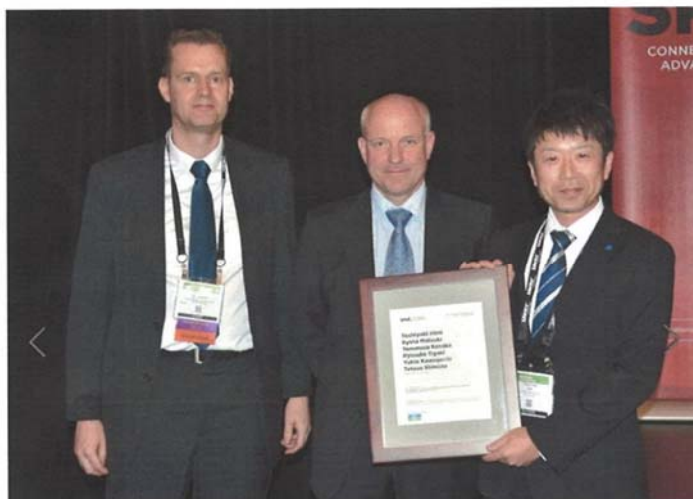


Figure 41. DSA ECOSYSTEM INTERACTION

14. Award and Honors

Awards and Honors



JEFFREY BYERS MEMORIAL BEST POSTER AWARD

THE 2017 JEFFREY BYERS MEMORIAL BEST POSTER AWARD WAS PRESENTED TO TOSHIYUKI HIMI (RIGHT) BY ADVANCES IN PATTERNING MATERIALS AND PROCESSES XXXV CONFERENCE CHAIR CHRISTOPH HOHLE (CENTER) AND CO-CHAIR ROEL GRONHEID (LEFT). AWARD SPONSORED BY TEL.

Figure 42. JEFFREY BYERS MEMORIAL BEST AWARD at SPIE

Figure 42 shows the awarding of the JEFFREY BYERS MEMORIAL BEST AWARD at SPIE to Himi and his collaborators. It was a short time after I started teaching anionic polymerization technology to Horiba's engineers, and I am sincerely grateful for their hard work. The following is a list of the years and the number of times “Horibanian”, Himi and his colleagues, presented their research at international conferences.

■DSA International Symposium: 6 times from 2015~2018

■SPIE: 4 times between 2016~2019

■Photopolymer Conference: 3 times during the period 2016~2018

Apart from this, we have collaborated with Hitachi Chemical, Nagoya University and Nippon Paul to present our work at DSA International Conference 3 times.

15. Comparison with other companies' products (reference data)

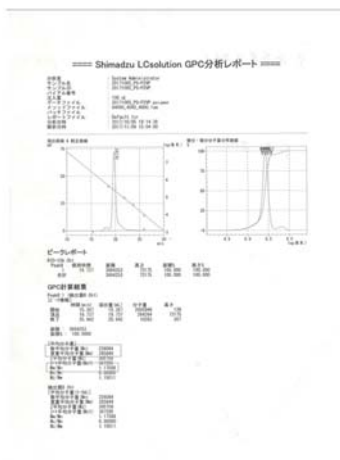


Figure 43. GPC chart of purchased P(St-*b*-2VP)

Figure 43 shows a GPC chart of P(St-*b*-2VP) purchased from a polymer manufacturer. It is presented here for reference.

16. Appendix ALD studies



Figure 44. TMI direct feed system

Figure 44 is the world's first direct feed system for MOCVD materials developed by me. It was especially effective in precisely feeding TMI (Trimethyl indium), which is solid at room temperature. This system has been on the market since January 1989 and is still in operation at several semiconductor companies. This equipment can also be used to supply ALD raw materials.

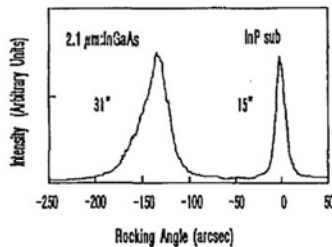
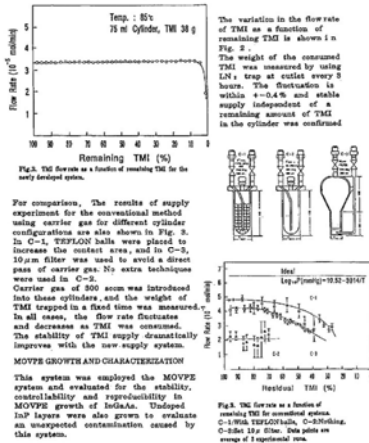


Fig. 4. Rocking curve of InGaAs/InP.

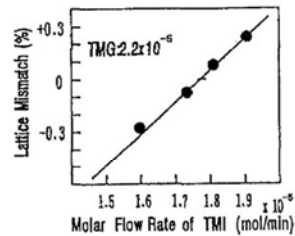


Fig. 6. Lattice mismatch as a functional TMI flow rate.

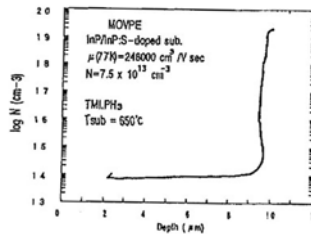
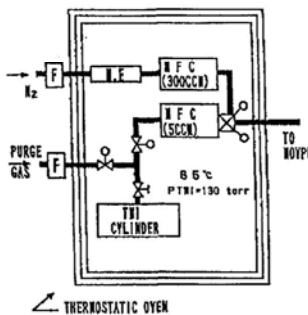
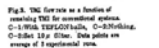


Fig. 7. Typical electrochemical peralson profile of an InP epilayer

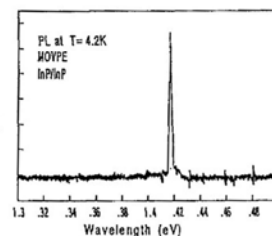


Fig. 8. Photoluminescence spectrum of an InP epilayer at 4.2K

Hirahara et al., 3rd International Conference on Indium Phosphide and Related Material, 640, 1991

Figure 45. Equipment Overview and Epi Data

17. ALD (Atomic Layer Deposition)

Niwano and Hirose are world authorities in ALD research. In particular, Hirose has conducted detailed research on the adsorption and oxidation mechanisms of raw materials for high-k, as well as the decomposition and stacking processes of raw materials, and has achieved numerous research results. [40]~[58]

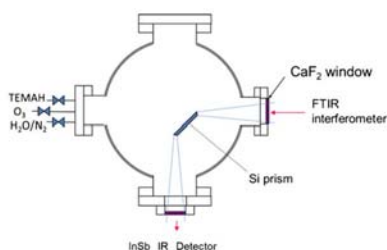


Figure 46. Schematic diagram of ALD chamber

AB-doped Si (100) substrate with a resistivity of approximately 10 Ωcm was used the sample. The same sample was introduced a stainless steel vacuum chamber for ALD with facilities for infrared absorption spectroscopy (IRAS) with a multiple internal reflection (MIR) geometry as a directed in situ, as shown in Figure 46.

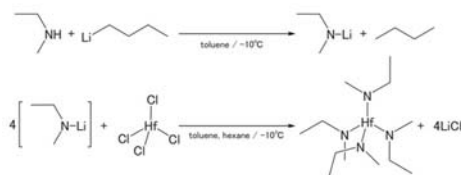


Figure 47. Synthesis method of TEMAH

We started with basic research on high-k raw materials such as TDMAS, TEMAH (Figure 47), and TEMAZ, and eventually established mass production technology using 500-5000L reaction vessels. We also developed a 50 kg scale feeder system to supply feedstock to ALD production machines, and delivered it to a semiconductor manufacturer. Figure 48 compares the V_g -leakage characteristics of an ultra-pure TEMAH (P-TEMAH) synthesized using my original purification method with those of a HfO₂ capacitor made with average commercial s-TEMAH.

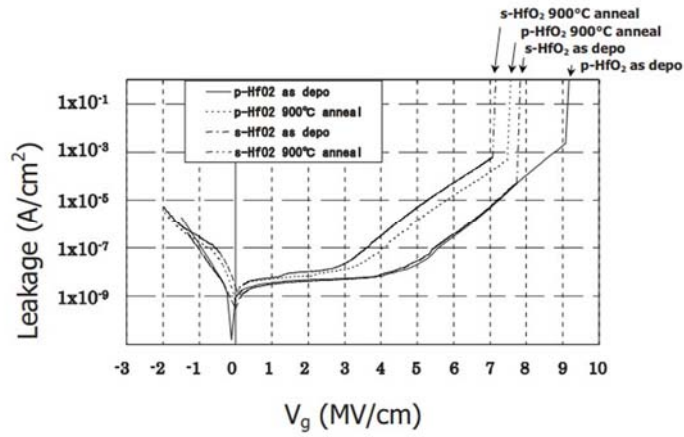


Figure 48. V_g -leakage characteristics for HfO_2 capacitor

High-purity TEMAH was synthesized by a chemical refinement and distilling method using ethylmethylaminolithium and hafnium tetrachloride. It is possible to reduce impurities in HfO_2 film by reducing the impurities in the hafnium raw material. And, the reduction efficiency in the HfO_2 film is proportional to the reduction number in the raw material. Electrical evaluation using high-purity TEMAH showed a low leakage current and low CFT value before annealing.

18. Last but not least

We believe that the final form of semiconductor lithography is EUV + DSA + ALD, but NIL + DSA + ALD may well be possible if for some reason EUV equipment cannot be purchased.

19. REFERENCES

- [1] G. E. Molau in "Block Copolymers", S. L. Agarwal, Ed; Plenum Publishing Corporation, New York, N.Y.,1970.
- [2] A. Norshay and J. E. McGrath, 'Block Copolymers' in "Overview and Critical Survey", Academic Press Inc., New York, N.Y., 1977.
- [3] G. Riess, "Encycl. Polym. Sci. and Eng.", John Wiley & Son, Inc., New York, N.Y., 1986. [4] B. R. M. Gallot, Adv. Polym. Sci., 1978, 29, 85
- [5] Caille, A. C.R. Hebd. Sean. Acad. Sci. 1972, 274, 891.
- [6] Herr, D. J. C. J. Mater. Res. 2011, 26, 122
- [7] Park, C.; Yoon, J.; Thomas, E. L. Polymer 2003, 44, 7779.
- [8] Segalman, R. A. Mater. Sci. Eng. R 2005, 48, 191
- [9] A. Takano, K. Soga, J. Suzuki and Y. Matsushita, Macromolecules 2003, 36, 9288-9291 [10] A. Takano, K. Soga, T. Asari, J. Suzuki, S. Arai, H. Saka and Y. Matsushita, Macromolecules 2003, 36, 8216-8218
- [11] A. Takano, S. Sato, T. Araki, K. Hirahara, S. Kawahara, Y. Isono, A. Ohno, N. Tanaka and Y. Matsushita, Macromolecules 2004, 37, 9941-9946
- [12] A. Takano, W. Kawashima, A. Noro, Y. Isono, N. Tanaka, T. Dotera and Y. Matsushita, J. Polym. Sci. Part B, Polym. Phy. 2005, 43, 2427-2432
- [13] K. Hayashida, W. Kawashima, A. Takano, Y. Shinohara, Y. Amemiya, Y. Nozue and Y. Matsushita, Macromolecules 2006, 39, 4869-4872.
- [14] K. Hayashida, T. Dotera, A. Takano and Y. Matsushita, Phys. Rev. Lett. 2007, 98 (19), 195502
- [15] K. Hayashida, A. Takano, T. Dotera and Y. Matsushita, Macromolecules 2008, 41, 6269-6271
- [16] K. Se, H. Yamasaki, A. Takano, and T. Fujimoto, Macromolecules 1997, 30(6), 1570-1576
- [17] T. Fujimoto, K. Ohkoshi, Y. Miyaki, and M. Nagasawa, Science, 1984, 224, 74
- [18] H. Funabashi, Y. Miyamoto, Y. Isono, T. Fujimoto, Y. Matsushita, M. Nagasawa, Macromolecules, 1983, 16,(1)
- [19] Y. Isono, H. Tanisugi, K. Endo, T. Fujimoto, H. Hasegawa, T. Hashimoto, H. Kawai, Macromolecules 1983, 16, 5-10
- [20] K. Hirahara, S. Takahashi, M. Iwata, T. Fujimoto, Y. Miyaki, Ind. Eng. Chem. Prod. Res. Dev. 1986, 25, 305

- [21] Y. Isono, K. Hirahara, H. Ito, T. Fujimoto, Y. Miyaki, J. Memb. Sci. 1989, 43, 205
- [22] K. Se, K. Miyawaki, K. Hirahara, A. Takano, T. Fujimoto, J. Polym. Sci.: Part A: Polym. Chem., 1998, 36, 3021
- [23] K. Hirahara, O. Watanabe, A. Takano, and Y. Isono, Reactive & Functional Polym. 1998, 37, 169-182
- [24] C. Wang, T. Sakai, O. Watanabe, K. Hirahara, T. Nakanishi, J. Electrochem. Soc., 2003 150, (9) A1166
- [25] O. Watanabe, K. Hirahara, T. Nakanishi, ACS meeting, Div. of Polymer Chemistry, 37, No. 2, 690 (1996)
- [26] K. Hirahara, M. Ueno, O. Watanabe, T. Nakanishi, M. Yamada, 9th International Meeting on Lithium Batteries, July (1998) {Invited speaker}
- [27] K. Hirahara, M. Ueno, O. Watanabe, T. Nakanishi, 10th International Meeting on Lithium Batteries, May (2000)
- [28] D. Baril, T. Nakanishi, K. Hirahara, O. Watanabe, M. Ueno, M. Armand, 3rd Hawaii Meeting on Lithium Batteries,
- [29] Y. Kawaguchi, T. Kosaka, T. Himi, K. Hirahara, 1st International Symposium on DSA, October (2015)
- [30] A. Takano, O. Kadoi, K. Hirahara, S. Kawahara, Y. Isono, J. Suzuki, Y. Matsushita, Macromolecules, 2004, 37(26), 9941
- [31] T. Kosaka, Y. Kawaguchi, T. Himi, T. Shimizu, K. Hirahara, A. Takano and Y. Matsushita, Proc. of SPIE 9779 977916 (2016)
- [32] T. Himi, Y. Kawaguchi, T. Kosaka, K. Hirahara, A. Takano and Y. Matsushita, Journal of Photopolymer Science and Technology 29, Number 5 (2016)
- [33] A. Takano, K. Hirahara, M. Takakuwa, K. Yamada, Y. Matsushita, 2nd International Symposium on DSA, (2016)
- [34] T. Umeda, K. Hirahara, Y. Matsushita, A. Takano, T. Murakami, S. Tsuzuki, 3rd International Symposium on DSA (2017)
- [35] K. Aizu, K. Watanabe, K. Watanabe, K. Hirahara, A. Takano, Y. Matsushita, 4th international Symposium on DSA (2018)
- [36] EE Times, Fukuda et. al.
<https://eetimes.itmedia.co.jp/ee/articles/2012/18/news027.html>
- [37] Semiconductor Engineering
<https://semien.gineering.com/directed-self-assembly-gets-another-look/>
- [38] A. Takano, O. Kadoi, K. Hirahara, S. Kawahara, Y. Isono, J. Suzuki and Y. Matsushita, Macromolecules, 2023, 36, 3045-3050
- [39] A. Takano, A. Nomura, O. Koide, K. Hirahara, S. Kawahara, Y. Isono, N. Torikai, Y. Matsushita,

Journal of Polymer Science, Part B. Polymer Physics 2002

- [40] Y. Kinoshita, F. Hirose, H. Miya, K. Hirahara, Y. Kimura, and M. Niwano, *Electrochemical Solid-state letters*, 10, (10), G80-G83 2007
- [41] H. Miya, M. Asai, K. Hirahara, Y. Kinoshita, and F. Hirose, *Electrochemical and Solid-State Letters*, 11, (7), 2008
- [42] F. Hirose, Y. Kinoshita, H. Miya, K. Hirahara, Y. Kimura, M. Niwano, 3rd International Work-Shop on New Group IV semiconductor Nanoelectronics 2007
- [43] F. Hirose, Y. Kinoshita, H. Miya, K. Hirahara, Y. Kimura, M. Niwano, 3rd International Work-Shop on New Group IV Semiconductor Nanoelectronics 2007
- [44] F. Hirose, Y. Kinoshita, H. Miya, K. Hirahara, Y. Kimura, M. Niwano, 3rd International Work-Shop on New Group IV Semiconductor Nanoelectronics 2007
- [45] F. Hirose, Y. Kinoshita, K. Hirahara, T. Shibuya, T. Suzuki, Y. Kimura, *ECS transaction*, 13, 171, 2008
- [46] F. Hirose, Y. Kinoshita, T. Shibuya, H. Miya, K. Hirahara, Y. Kimura, M. Niwano, *ECS transaction*, 19, 417, 2009
- [47] F. Hirose, Y. Kinoshita, S. Shibuya, H. Miya, K. Hirahara, Y. Kimura, M. Niwano, *Thin Solid Film*, 519, 270, 2010
- [48] M. Degai, K. Kanomata, K. Komiyama, K. hirahara, S. Kubota, F. Hirose, *Thin Solid Film*, 525, 73, 2012
- [49] F. Hirose, Kinoshita, K. Kanomata, K. Hirahara, K. Momiyama, S. Kubota, K. Kimura, M. Niwano, *Applied Surface Science*, 258, 7726, 2012
- [50] K. Kanomata, P. Pansila, B. Ammad, K. Hirahara, F. Hirose, *Applied Surface Science*, 308, 328, 2014
- [51] J. Hidaka, A. Yamaguchi, K. Hirahara, 3rd International Conference on Indium Phosphide and Related Material, 640, 1991
- [52] F. Hirose, Y. Kinoshita, H. Miya, K. Hirahara, Y. Kimura, M. Niwano, *ALD*, 2006
- [53] F. Hirose, Y. Kinoshita, H. Miya, K. Hirahara, Y. Kimura, M. Niwano, 5th International Symposium on Control of Semiconductor Interface, 2007
- [54] F. Hirose. Y. Kinoshita, H. Miya. K. Hirahara, Y. Kimura, M. Niwano, 5th International Symposium on Control of Semiconductor Interface, 2007
- [55] F. Hirose, Y. Kinoshita, T. Shibuya, K. Hirahara, T. Suzuki, Y. Kimura, M. Niwano, 213th Meeting of the electrochemical society 2008
- [56] F. Hirose, Y. Kinoshita, T. Shibuya, H. Miya, K. Hirahara, Y. Kimura, M. Niwano, 215th Meeting of the electrochemical society 2009
- [57] K. Kanomata, K. Moriyama, K. Hirahara, S. Kubota, F. Hirose, 223th Meeting of the electrochemical society 2013

[58] K. Kanomata, T.Suzuki, B. Ahmmad, K. Hirahara, S. Kubota, T. Takeda, F. Hirose, 2013 Asia-Pacific Work-shop of Fundamentals and Application of Advanced Semiconductor Device 2013

[59]Sin-Etsu MicroSi

<https://www.microsi.com/blog/directed-self-assembly/>